The Functional Neuroanatomy of Target Detection: An fMRI Study of Visual and Auditory Oddball Tasks

David E.J. Linden[1,2,3], David Prvulovic[2], Elia Formisano[4], Martin Völlinger[4], Friedhelm E. Zanella[4], Rainer Goebel[1] and Thomas Dierks[2,5]

[1]Max-Planck-Institut für Hirnforschung, Frankfurt am Main, [2]Department of Psychiatry, Division of Clinical Neurophysiology, [3]Department of Neurology and [4]Department of Neuroradiology, Johann Wolfgang Goethe-Universität, Frankfurt am Main, Germany and [5]Department of Psychiatry, University of Bern, Switzerland

The neuronal response patterns that are required for an adequate behavioural reaction to subjectively relevant changes in the environment are commonly studied by means of oddball paradigms, in which occasional 'target' stimuli have to be detected in a train of frequent 'non-target' stimuli. The detection of such task-relevant stimuli is accompanied by a parietocentral positive component of the event-related potential, the P300. We performed EEG recordings of visual and auditory event-related potentials and functional magnetic resonance imaging (fMRI) when healthy subjects performed an oddball task. Significant increases in fMRI signal for target versus non-target conditions were observed in the supramarginal gyrus, frontal operculum and insular cortex bilaterally, and in further circumscribed parietal and frontal regions. These effects were consistent over various stimulation and response modalities and can be regarded as specific for target detection in both the auditory and the visual modality. These results therefore contribute to the understanding of the target detection network in human cerebral cortex and impose constraints on attempts at localizing the neuronal P300 generator. This is of importance both from a neurobiological perspective and because of the widespread application of the physiological correlates of target detection in clinical P300 studies.

Introduction

In natural environments, sudden change of the perceived surroundings often threatens the individual's physical integrity. The rapid detection of relevant changes of the external sensory stimulation and the execution of adequate behavioural responses can therefore be crucial for survival. On the other hand, adaptation to regularly occuring stimuli and extrapolation of future events confers economic benefits that might be equally important. The allocation of resources to the detection of mismatches therefore involves a tradeoff between attentional economy and the potential need for rapid responses.

The neuronal correlates of the detection of subjectively relevant information are commonly studied with 'oddball' paradigms, in which occasional relevant ('target') stimuli that require a specific cognitive response have to be detected in a train of frequent irrelevant 'non-target' stimuli. The detection of targets in an oddball paradigm is associated with an event-related potential component ~300–500 ms post-stimulus (Ritter and Vaughan, 1969), depending on stimulus modality. This task-related parietocentral component (Vaughan and Ritter, 1970) has been named 'P3' (Smith *et al.*, 1970), 'P300' (Ritter *et al.*, 1968) or 'late positive component' (Sutton *et al.*, 1965). Its amplitude increases with target improbability (Squires *et al.*, 1976) and interstimulus interval (Polich, 1990; Polich *et al.*, 1991), while the latency depends on the difficulty of the task [reviewed by Picton (Picton, 1992)]. The amplitude, latency and topography of the P300 are furthermore altered in a number of neuropsychiatric disorders, such as schizophrenia (Strik *et al.* 1994; Pritchard, 1986), autism (Oades *et al.*, 1988), dementia (Goodin *et al.*, 1978; Dierks and Maurer, 1990), metabolic encephalopathies (Davies *et al.*, 1990) and alcoholism (Pfefferbaum *et al.*, 1979). The amplitude of the P300 is also reduced by focal cortical lesions, particularly of the temporoparietal junction (Knight *et al.*, 1989; Yamaguchi and Knight, 1992), but also of the frontal lobes (Yamaguchi and Knight, 1991).

Evidence as to the generators of the P300 wave has been obtained from lesion studies [reviewed by Knight (Knight, 1990)], intracerebral electrical recording in humans (Puce *et al.*, 1989; Smith *et al.*, 1990; Baudena *et al.*, 1995; Halgren *et al.*, 1995a,b) [reviewed by Halgren *et al.* (Halgren *et al.*, 1998)], cats (O'Connor and Starr, 1985) and monkeys (Paller *et al.*, 1988, 1992; Arthur and Starr, 1994), source localization studies of scalp electrical (Menon *et al.*, 1997) and magnetic (Basile *et al.*, 1997; Mecklinger *et al.*, 1998) evoked responses, and functional magnetic resonance imaging (fMRI) (Dierks *et al.*, 1997; McCarthy et al, 1997; Menon *et al.*, 1997).

Human lesion studies point mainly towards temporoparietal and frontal generators, while the intracranial recordings suggest an additional contribution of limbic and paralimbic areas. These two approaches, while providing the most direct access to the generators of the P300 wave, warrant cautious interpretation. Lesion studies, by definition, require previous damage to the brain and therefore do not necessarily provide a picture of the normal working brain. Similarly, intracranial recordings in humans can only be applied to certain groups of patients. Both methods have the additional disadvantage that they provide information only about a limited number of brain sites whose selection does not primarily depend on the experimental requirements, but on the clinical indication or type of lesion. It is therefore important to supplement the contribution of the lesion studies and intracranial recordings with non-invasive functional neuroimaging of the entire brain in healthy subjects. The reconstruction of sources of evoked magnetic fields has so far been only partially successful, perhaps owing to the nature of the generators, which are not easily treated as point sources (Halgren, 1998). fMRI alone (McCarthy *et al.*, 1997) and with EEG (Menon *et al.*, 1997) confirmed the contribution of temporoparietal and frontal areas to the oddball response. These functional imaging studies, however, covered only parts of the brain and did not test the effect of a variation of stimulus and response modalities. Therefore their design did not allow for a differentiation between modality-specific higher sensory functions and the intermodal network for target detection. Similarly, it was almost impossible to determine the extent to which the observed blood oxygen level-dependent (BOLD) signal changes could be attributed to specific effects of the type of response (mental counting or finger movements, respectively) the subjects had to make.

In the present whole-brain fMRI study of the oddball paradigm, we use both auditory and visual stimuli and mental

counting and button-press responses in order to obtain effects that are invariant for stimulation and response modality and can thus be regarded as functional imaging equivalents of the P300 component.

Materials and Methods

Subjects and Task

Five neurologically and mentally healthy male subjects (age range 25–37, mean 29) were recruited from an academic environment. All subjects gave informed consent to participation in the study. The four experimental conditions were defined by the mode of stimulus delivery (visual or auditory) and of the subjects' response (mental counting of targets or differential button press). All four conditions were tested in separate EEG and fMRI sessions. Stimuli were generated on a personal computer using the STIM® software package (Neuroscan, Inc., Hernon, USA). In the EEG setting, stimuli were presented using the STIM hardware for visual and auditory stimulation. In the fMRI setting, visual stimuli were delivered to a high luminance LCD projector (EIKI LC-6000), and auditory stimuli to a custom-made sound transmission device that accurately preserves tone frequencies.

The visual oddball paradigm consisted of sequences of angles that were presented for 800 ms every 8 s. Subjects had to detect small angles (15°) in trains of large angles (60°). The auditory oddball paradigm consisted of sine tones of 1000 and 2000 Hz at a sound pressure level of 90 dB that were presented for 200 ms (including 10 ms rise-time and 10 ms fall-time) every 8 s. The 2000 Hz tone was defined as target. In both paradigms, targets appeared in pseudo-random order with a probability of 15% and were separated from the next target by at least 32 s to allow for a return of the BOLD signal to baseline levels. In the button-press conditions, subjects had to press a button with the right index finger upon each stimulus presentation. One button was defined as target and another as non-target button. Responses were recorded using the STIM hardware (during EEG) and a custom-made fibreoptic answer-box (during fMRI). In the counting condition subjects silently counted the targets and reported the result after the session.

ERP Recording and Analysis

The event-related electric potentials were recorded using NeuroScan equipment with Synamps amplifiers (Neuroscan, Inc.). Twenty electrodes were placed according to the 10–20 System (Fp1, Fp2, F7, F3, Fz, F4, F8, T3, C3, C4, T4, T5, P3, Pz, P4, T6, O1, O2, A1, A2) and recorded against the electrode Cz as reference. Two additional bipolar pairs of electrodes were placed to record horizontal and vertical EOG, and one bipolar pair to record ECG. The ERPs were recorded as ongoing EEG and digitized with a rate of 512 Hz. Prior to digitizing the EEG was bandpass filtered at 0.1–30 Hz.

The analysed time epoch at each stimulation was 1024 ms (200 ms pre- and 824 ms post-stimulus). For each epoch a baseline correction for the data 200 ms prior to the stimulus was performed. To avoid artefacts all epochs containing data exceeding ±50 μV in any channel (except for ECG channels) were excluded from further analysis. For each condition, ~20 target sweeps were obtained free of artefacts. The average for each subject for each stimulus and response condition was calculated separately for target and non-target stimuli (4 × 2 conditions). The data were recalculated using linked mastoids as reference [(A1 + A2)/2]. To obtain topographical unbiased amplitude values, we computed the global field power (GFP) (Lehmann and Skrandies, 1971; Rodin 1991; Pritchard *et al*, 1996; Fylan *et al*, 1997). The maximal GFP amplitude was measured for the target stimuli in a time window of 300–400 ms for auditory and 400–600 ms for visual paradigms and compared to the GFP amplitude for non-target stimuli at the same time point (paired Student's *t*-test).

fMRI Measurements and Analysis

The MR scanner used for imaging was a 1.5 T whole-body superconducting system (MAGNETOM Vision, Siemens Medical Systems, Erlangen, Germany) equipped with a standard head coil, an active shielded gradient coil (25 mT/m) and echo planar sequences for ultra-fast MR imaging.

For functional imaging, we used a BOLD sensitive single-shot echo planar (EPI) sequence (T_E = 26 ms; T_R = 2000 ms; flip angle = 90°; matrix size = 64 × 64) and an event-related design with a time resolution of 2 s. Each functional volume consisted of 12 slices, with a thickness of 6 mm and a pixel size of 3.125 × 3.125 mm (field of view: 200 × 200 mm), located along oblique planes parallel to the plane crossing the anterior and posterior commissure.

Each functional time-series consisted of 128 volumes and lasted for 256 s. During this time 32 stimuli were presented at 8 s intervals. For each of the four conditions (visual oddball–counting; visual oddball–button press; auditory oddball–counting; auditory oddball–button press) four functional time series were acquired. Every subject thus underwent 16 scans of 128 volumes each.

For the three-dimensional reconstruction of functional data, high-resolution three-dimensional data sets [T_1 weighted FLASH (fast low-angle shot) with 180 partitions; isotropic voxel size 1 mm^3] were acquired for each subject.

Data analysis, registration and visualization were performed with the fMRI software package BrainVoyager 3.0 (Goebel *et al.*, 1998a,b, Dierks *et al.* 1999). Prior to statistical analysis, the time series of functional images was aligned for each slice in order to minimize the signal changes related to small motions of the subject during the acquisition. The realigned time series were spatially filtered by convolving each EPI image with a bidimensional Gaussian smoothing kernel with full width at half maximum (FWHM) = 2 pixels. No temporal smoothing was performed in order to maintain the single trial temporal resolution. Furthermore, the linear drifts of the signal with respect to time were removed from each pixel's time-course. The two-dimensional slice time-courses were then converted into three-dimensional volume time-courses by co-registration with the three-dimensional anatomical data sets that were acquired in the same scanning sessions.

Co-registration was based on the Siemens slice position parameters of the T_2*-weighted measurement (number of slices, slice thickness, distance factor, Tra–Cor angle, FOV, shift mean, off-centre read, off-centre phase, in-plane resolution) and of the T_1-weighted FLASH measurement (number of sagittal partitions, shift mean, off-centre read, off-centre phase, resolution) with respect to the initial overview measurement (scout).

For each subject the structural and functional three-dimensional data sets were transformed into Talairach space. Talairach transformation was performed in two steps. The first step consisted in rotating the three-dimensional data set of each subject to be aligned with the stereotaxic axes. For this step the location of the anterior commissure (AC) and the posterior commissure (PC) and two rotation parameters for midsagittal alignment had to be specified manually in the three-dimensional FLASH data set. In the second step the extreme points of the cerebrum were specified. These points together with the AC and PC coordinates were then used to scale the three-dimensional data sets into the dimensions of the standard brain of the Talairach and Tournoux atlas (Talairach and Tournoux, 1988) using a piecewise affine and continuous transformation for each of the 12 defined subvolumes.

The statistical analysis of the variations of the BOLD signal was based on the application of the general linear model to time series of task-related functional activation (Holmes *et al.* 1997). General linear models were computed for each of the four conditions from 20 volume time-courses (five subjects, four repetitions) with 128 time points each. The design matrix contained the 20 idealized response functions (assuming the value 1 for the four time points following the presentation of the target and the value 0 for the remaining time points) that corresponded to these signal time-courses. For statistical analysis, any combination of predictors can be used. It is thus possible to compute both single subject and group effects and to test for inter- and intraindividual stability. In the present study, the identification of task-related spatial activation patterns and comparison between the four task conditions was based on group correlation maps (five subjects, four repetitions of 128 time points each per condition) thresholded at $r > 0.4$ ($P < 10^{-4}$, uncorrected).

In order to exclude a confounding effect of sample size differences we performed a second analysis of the volume time-courses, in which the specified predictor for the target epochs was compared to a baseline condition of equal length (the baseline predictor included the four time points prior to each target). Effects were only accepted as significant when they were specific for the target versus baseline epochs at $P < 10^{-4}$

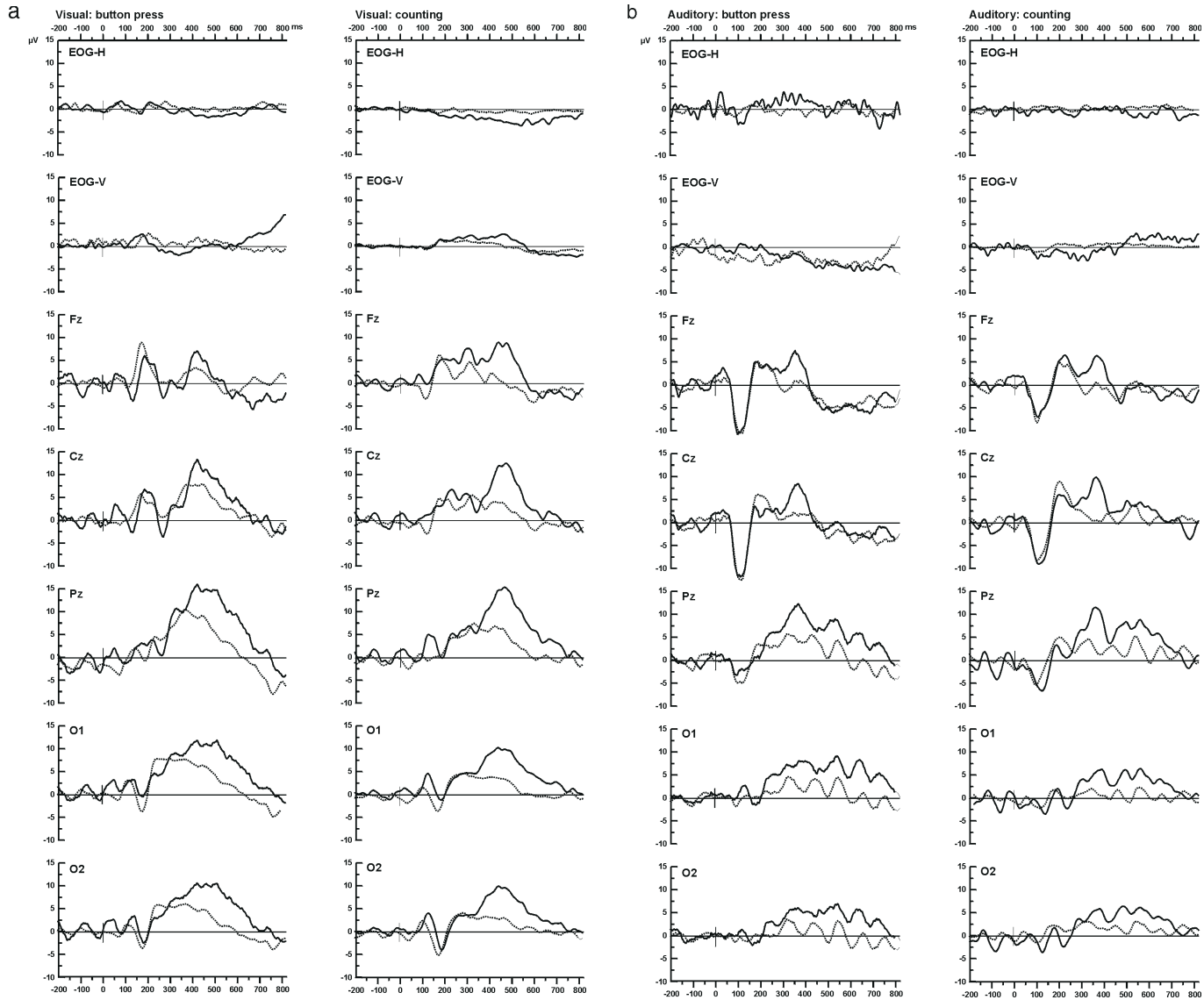

Figure 1. Average ($n = 5$) ERP wave forms at scalp electrodes Fz, Cz, Pz, O1 and O2 and for horizontal (EOG-H) and vertical (EOG-V) electrodes for targets (solid line) versus non-targets (dotted line) in all stimulation and response modalities (*a*, visual; *b*, auditory stimulation). The button-press reaction times were greater for targets than for non-targets (auditory target 706 ms, SD 158 ms; auditory non-target 530 ms, SD 131 ms; visual target 611 ms, SD 118 ms; visual non-target 525 ms, SD 116 ms). The error rates were 1.8% for visual button press and 1.1% for auditory button press.

and the baseline predictor did not show any significant departure from the overall average of the time-course.

The T_1-weighted FLASH three-dimensional recording of one subject was used for a surface reconstruction of both hemispheres. The white/grey matter border was segmented with a region-growing method. The discrimination between white and grey matter was improved by several manual interactions (e.g. labelling subcortical structures as 'white matter'). The white/grey matter border was finally tesselated in a single step using two triangles for each side of a voxel located at the margin of white matter. The tesselation of a single hemisphere typically consists of roughly 240 000 triangles. The reconstructed surface is subjected to iterative corrective smoothing (100–200 iterations). An interactive morphing algorithm (Goebel *et al.*, 1998a) was used to let the surface grow smoothly into the grey matter. Through visual inspection, this process was halted when the surface reached the middle of grey matter (approximately layer 4 of the cortex). The resulting surface was used as the reference mesh for the visualization of functional data. The iterative morphing algorithm was further used to inflate each hemisphere. An inflated hemisphere possesses a link to the folded reference mesh so that functional data may be shown at the correct position of the inflated representation. This link was also used to keep geometric distortions during inflation to a minimum with a morphing force that keeps the area of each triangle of the inflated hemisphere as close as possible to the value of the folded reference mesh. This display of functional maps on an inflated hemisphere allows the topographic representation of the

Table 1
Mean and standard deviation (SD) for P300 GFP amplitudes for targets and non-targets in all stimulation and response modalities

	Visual				Auditory			
	Button press		Counting		Button press		Counting	
	Target	Non-target	Target	Non-target	Target	Non-target	Target	Non-target
Mean (μV)	7.37	3.55	4.92	2.27	5.15	2.27	3.70	1.76
SD	2.38	1.68	0.69	0.97	2.16	0.99	1.02	0.59
P	<0.001		0.036		0.013		0.004	

Table 2

Anatomical areas (for abbreviations see Talairach and Tournoux, 1988) and Brodmann areas (BA) of activated clusters in the four experimental conditions and Talairach coordinates (Talairach and Tournoux, 1988) of centres of mass of group and (in brackets) single subject clusters

Experiment	Anatomical area	BA	*x*	*y*	*z*	*n*
Visual stimulus, button press	right Gsm	40	52 (48 ± 4.6)	–31 (–34 ± 6.2)	41 (41 ± 5.9)	5
	left Gsm	40	–49 (–52 ± 1.8)	–24 (–29 ± 4.1)	46 (42 ± 5.8)	4
	right sylvian	45/insula	48 (47 ± 3.6)	4 (6.4 ± 5.6)	11 (9 ± 4.4)	5
	left sylvian	45/insula	–45 (–40 ± 4.8)	–2 (1 ± 6.0)	10 (9 ± 4.3)	5
	SMA/ant. GC	32	–1 (1 ± 6.3)	–1 (2 ± 4.6)	46 (46 ± 1.3)	4
	right VC	17/18	14 (13 ± 2.6)	–96 (–93 ± 1.7)	5 (5 ± 6.2)	5
Visual stimulus, silent counting	right Gsm	40	55 (56 ± 2.2)	–36 (–31(4.7)	35 (31 ± 2.9)	4
	left Gsm	40	–55 (–53 ± 5.5)	–37 (–34 ± 7.5)	33 (35 ± 2)	3
	right Sylvian	45/insula	44 (47 ± 4.4)	9 (6.2 ± 5.0)	9 (8.6 ± 4.9)	5
	left sylvian	45/insula	–42 (–41 ± 6.1)	2 (0 ± 10.0)	8 (8.2 ± 5.2)	5
	SMA/ant. GC	32	0 (3 ± 2.7)	5 (6 ± 4.9)	46 (41 ± 3.6)	5
	right VC	17/18	15 (11 ± 5.5)	–96 (–90 ± 5.8)	7 (8 ± 4.6)	5
	right Lpi	40	41 (46 ± 4.5)	–29 (–32 ± 3.5)	48 (46 ± 1.2)	3
	left Lpi	40	–46 (50 ± 3)	–39 (–30 ± 3.4)	46 (48 ± 1.7)	4
Auditory stimulus, button press	right Gsm	40	55 (55 ± 4.0)	–33 (–31 ± 7.0)	31 (32 ± 7.2)	5
	left Gsm	40	–55 (–57 ± 3.7)	34 (–36 ± 6.4)	33 (36 ± 6.1)	5
	right sylvian	45/insula	42 (45 ± 4.6)	2 (2.6 ± 4.7)	–3 (5.2 ± 6.8)	5
	left sylvian	45/insula	–40 (–39 ± 1.4)	0 (1 ± 4.6)	0 (2 ± 4.4)	4
	bilateral Pcu	7	–2 (–5 ± 5.5)	–71 (–69 ± 2.3)	45 (42 ± 3.1)	3
	left GPoC	1/2/3	–50 (–45 ± 4.9)	–28 (–23 ± 4.2)	44 (45 ± 3.9)	4
Auditory stimulus, silent counting	right Gsm	40	55 (54 ± 5.8)	–29 (–29 ± 2.8)	26 (28 ± 2.6)	4
	left Gsm	40	–58 (–54 ± 3.7)	–40 (–36 ± 6.7)	27 (26 ± 6.6)	5
	right Sylvian	45/insula	43 (47 ± 4.7)	11 (11 ± 6.5)	–4 (0 ± 6.2)	5
	left Sylvian	45/insula	–39 (–42 ± 8.8)	11 (11 ± 10.2)	–4 (0 ± 5.4)	5
	SMA/ant. GC	32	0 (0 ± 2.4)	7 (6 ± 7.3)	44 (43 ± 3.7)	4
	post. GC	23	0 (3 ± 3.4)	–28 (–31 ± 4.1)	27 (33 ± 8.8)	5
	right Gfm	6	45 (45 ± 2.4)	1 (1.4 ± 3.1)	44 (44 ± 1.9)	5
	right Gtm	21	58 (51 ± 7.1)	–39 (–42 ± 4.0)	8 (9 ± 3.2)	3

For details of cluster selection, see Materials and Methods. The last column indicates for how many of the five subjects the activation reached significance at the $P < 10^{-4}$ (uncorrected) level. Only significant activations were used to compute SDs of single subject data. Note that in at least two directions of the Talairach coordinate system, activated clusters in BA40 and BA45/insula did not differ by more than 1 SD between experimental conditions (the largest variability being apparent along the *z*-axis).

three-dimensional pattern of cortical activation without loss of the lobular structure of the telencephalon.

Results

The evoked electric responses to the visual and auditory stimuli for the different response modalities, shown in Figure 1, reveal that the stimuli, which were identical for the EEG and fMRI measurements, had the properties of classical oddball paradigms. They elicited a marked parietocentral positivity at latencies of 400–550 ms (visual) and 300–400 ms (auditory) with significant GFP amplitude differences for targets versus non-targets (Table 1). The corresponding increases of the BOLD signal, measured with fMRI, for response to targets versus response to non-targets that were significant at the $P = 10^{-4}$ level (uncorrected) are summarized in Table 2 and presented as functional group data on inflated individual hemispheres in Figures 2 and 3. For all stimulation and response conditions, activation was consistently observed in bilateral perisylvian areas, including the supramarginal gyrus (BA 40), the frontal operculum (BA 45), and the insula. In all conditions except the auditory button-press, prominent activation was also observed in the frontal midline areas supplementary motor area (SMA) and anterior cingulate gyrus (BA 32). Additional clusters of activation appeared in primary and secondary visual cortex (BA 17/ 18) during the visual target presentation, in left Rolandic cortex (BA 1/2/3), the precuneus (BA 7) and the right middle temporal gyrus (BA 21) during the button press response to auditory targets, and in the posterior cingulate gyrus (BA 23) and the right middle frontal gyrus (BA 6) during the mental counting of auditory targets. The relative BOLD signal change for targets compared to a non-target baseline, averaged over all five subjects, peaked at ~0.4% (Fig. 4).

Discussion

The detection of rare target stimuli in a train of standard stimuli was associated with a prominent activation of bilateral perisylvian areas in the inferior parietal and frontal lobes and insular cortex. This activation was consistent over stimulation and response conditions and cannot be explained by specific effects of mental counting or motor response preparation, or the processing of visual or auditory stimuli, respectively. It was elicited by stimuli whose physical difference from the non-target stimuli was marginal, and which were characterized by their task-relevance and their frequency in the stimulus train. The activation of these perisylvian areas during the target epochs of different oddball tasks therefore suggests an involvement of these areas in the higher-order multimodal processing of sensory information that is modulated by the requirements of a cognitive task. According to this interpretation, the supramarginal gyrus, frontal operculum and insula would form a network for saliency detection in different sensory modalities. The frontal midline areas SMA and anterior cingulate have been shown to be involved in a wide variety of cognitive tasks and associated with effort and task difficulty (Dehaene *et al.*, 1998a; Paus *et al.*, 1998). Their activation during target detection in oddball paradigms might therefore reflect their general role in response

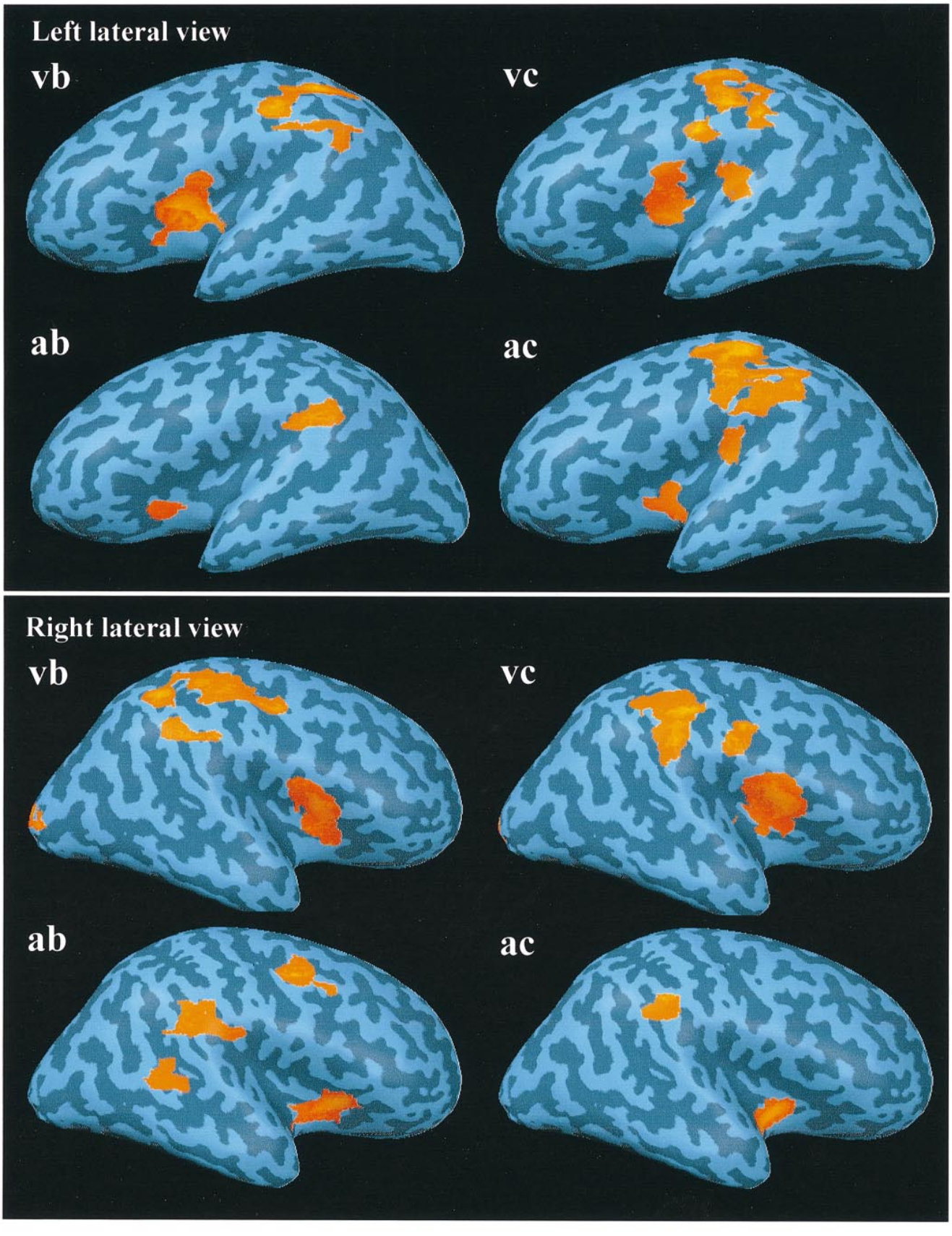

Figure 2. Average ($n = 5$) three-dimensional maps of BOLD signal increase for targets versus non-targets in all stimulation and response modalities superimposed on the inflated hemispheres of a single subject (see Materials and Methods). Lateral views. vb, visual stimulation–button press; vc, visual stimulation–counting; ab, auditory stimulation–button press; ac, auditory stimulation–counting.

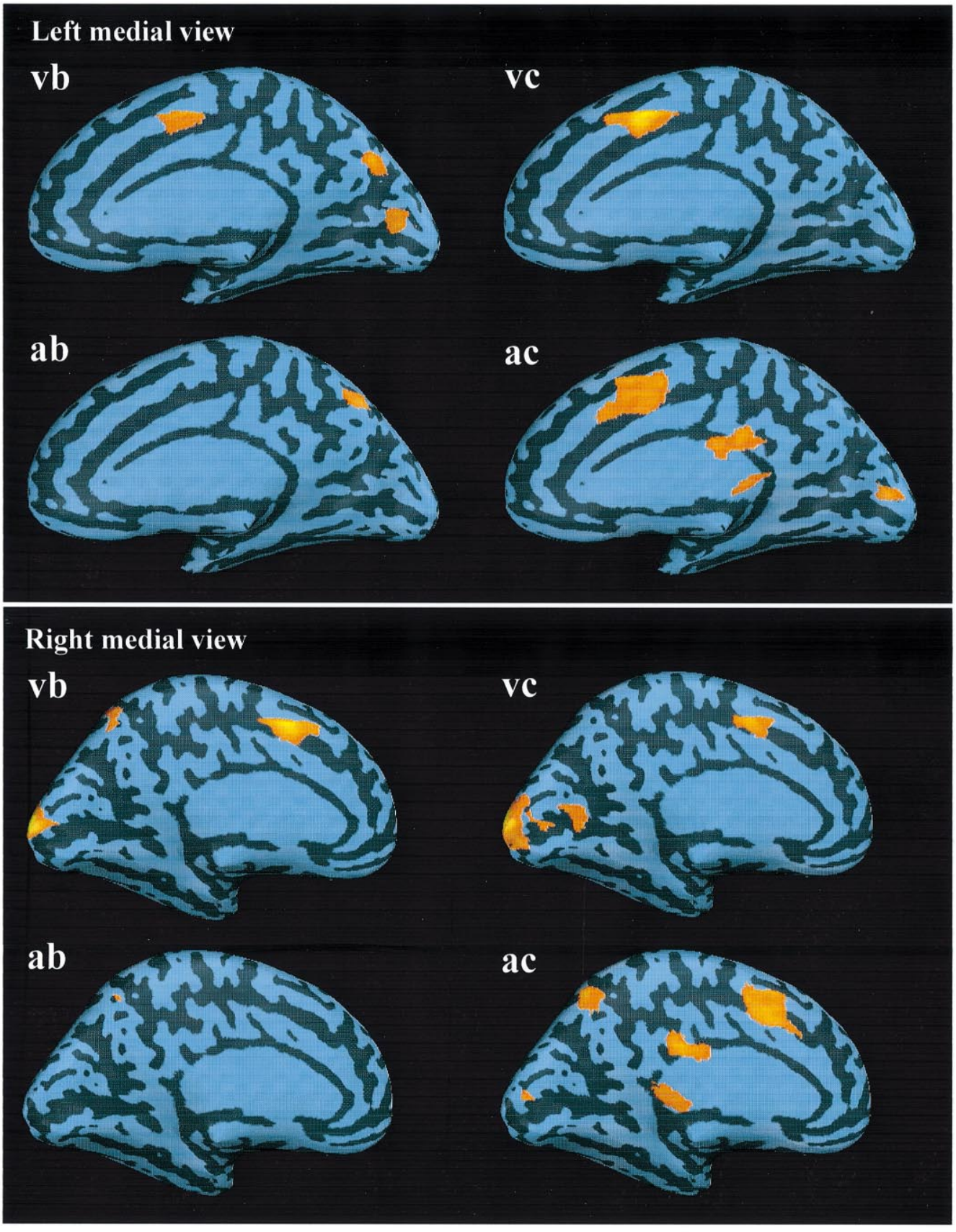

Figure 3. Average ($n = 5$) three-dimensional maps of BOLD signal increase for targets versus non-targets in all stimulation and response modalities superimposed on the inflated hemispheres of a single subject (see Materials and Methods). Medial views. The four conditions are coded as in Figure 2.

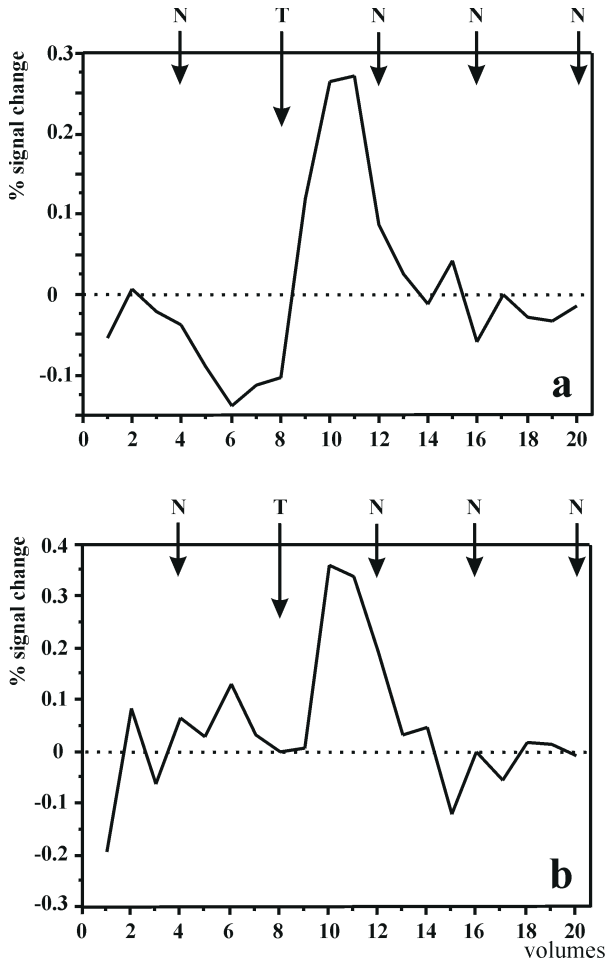

Figure 4. Average ($n = 5$; 512 time points each) time-courses of the BOLD response during target epochs (T) and the preceding and following non-target (N) epochs. The examples are drawn from the SMA (*a*) and the frontal operculum (*b*).

preparation in cognitive tasks and the monitoring of task-relevant information (Carter *et al.*, 1998).

Target detection did not elicit a very strong differential response in unimodal sensory cortex. Some activation was observed in primary and secondary visual areas during the detection of visual targets. This activation might reflect the attentive or pre-attentive modulation of early sensory processing, which has been suggested to occur already at the level of the striate cortex (Roelfsema *et al.*, 1998; Tootell *et al.*, 1998; Watanabe *et al.*, 1998; Yen and Finkel, 1998; Gandhi *et al.*, 1999). On the other hand, the activity of the the middle temporal gyrus, an area that has been implicated in the memory formation for auditory stimuli (Elger *et al.*, 1997), that was observed in the counting condition of the auditory oddball paradigm might be related to the process of updating the auditory input sequence.

It also seems that there was little activity that can be explained by specific effects of the response conditions. With regard to the button-press response, we modified the commonly used task requirements in order to make the paradigm suitable for fMRI. Subjects had to press a button whenever a stimulus appeared. One button coded for non-targets and another for targets. We still found a marked P300 effect for the rare targets, while avoiding the confound of finger movement-related activity that might be tolerable in scalp P300 applications, but had obscured the results of a number of earlier fMRI and source localization studies. The activity of the postcentral gyrus in the button-press condition of the auditory oddball paradigm might reflect the somatosensory component of the motor response, but no significant differential activation was observed in the motor cortex proper. An area extending from the angular gyrus to the intraparietal region, which might be involved in mental arithmetic [reviewed by Dehaene *et al.* (Dehaene *et al.*, 1998b)], was activated bilaterally during the counting condition of the visual, but not of the auditory oddball paradigm.

The localization of the components of the network for target detection in oddball tasks that is demonstrated by the present study matches lesion data (Knight *et al.*, 1989) and some of the sites suggested by intracranial recordings as generators of the P3. Halgren *et al.* elicited triphasic peaks with a prominent P3 equivalent in the supramarginal gyrus of pre-surgical epilepsy patients using visual and auditory oddball paradigms (Halgren *et al.*, 1995a). A similar effect could be obtained in the posterior cingulate gyrus with an auditory oddball task. In our experiment, activation was observed in the supramarginal gyrus bilaterally and consistently over all stimulus and response conditions (Table 2). The posterior cingulate, on the other hand, was significantly activated only during the silent counting of auditory oddballs (Table 2). In all of our conditions, except the button press to auditory rare targets, the anterior cingulate cortex (BA 32) was significantly activated (Table 2). This area was also found to be a generator of P3 waves in an intracranial evoked potential study that employed only an auditory oddball task (Baudena *et al.*, 1995). However, the activity of other areas that have been identified as generators of the intracranial P3 to rare auditory and visual stimuli, most notably the hippocampal complex (Halgren *et al.*, 1995b), did not reach significance in the group analysis of our fMRI data. This lack of hippocampal activation might reflect differences in the sensitivity of the two methods. As suggested by McCarthy *et al.*, possible differences between the fMRI activation pattern and that of the intracranial electric recording might be explained by differences in the underlying patterns of neuronal activity (McCarthy *et al.*, 1997). While the P300 component of ERPs reflects a transient synchronized synaptic activity that occurs only for a brief period (from 300 to 500 ms post-stimulus, depending on stimulus modality), the changes in the BOLD response might be brought about by a prolonged sustained activity of the target detection network that is not revealed in the evoked electric or magnetic field because it is not time-locked or because the fields generated in the neurons are not similarly oriented. fMRI at high temporal resolution (Menon and Kim, 1999), preferably in conjunction with EEG/MEG recordings and a combination of both modalities for source analysis (Scherg *et al.*, 1999), is required in order to test this hypothesis.

Our study confirms the finding of previous fMRI studies that target detection in oddball tasks is related to BOLD signal increases in the supramarginal gyrus (Dierks *et al.*, 1997; McCarthy *et al.*, 1997; Menon *et al.*, 1997) and other inferior parietal areas (McCarthy *et al.*, 1997) and in frontal midline areas (Dierks *et al.*, 1997; Menon *et al.*, 1997). However, none of the previous studies reported activity in the frontal operculum and the insula. This might be explained by the limitation of image acquisition to selected brain areas in these studies.

The present study shows that whole-brain event-related fMRI can make an important contribution to the identification of the target detection network in the brain of healthy subjects. While the clarification of the nature of the correspondence between the BOLD signal increase in oddball conditions and the intra-

cranial and scalp P300 is the most immediate issue, one should also consider the use of event-related fMRI to supplement the numerous studies on the subcomponents of the P300 wave and their functional significance in the normal and pathological brain.

Notes

This study was supported by the Alzheimer Research Centre, Frankfurt am Main, Germany and Alzheimer Forschungs-Initiative e.V.

Address correspondence to Dr David E.J. Linden, Department of Psychiatry I, Division of Clinical Neurophysiology, Heinrich-Hoffmann-Straße 10, DE-60528 Frankfurt am Main, Germany. Email: linden@mpih-frankfurt.mpg.de.

References

Arthur DL, Starr A (1994) Task-relevant late positive component of the auditory event-related potential in monkeys resembles P300 in humans. Science 223:186–188.

Basile LFH, Rogers RL, Simos PG, Papanicolaou AC (1997) Magnetoencephalographic evidence for common sources of long latency fields to rare target and rare novel visual stimuli. Int J Psychophysiol 25:123–137.

Baudena P, Halgren E, Clarke JM, Heit G, (1995) Intracerebral potentials to rare target and distractor auditory and visual stimuli: 3. Frontal cortex. Electroenceph Clin Neurophysiol 94:251–264.

Carter CS, Braver TS, Barch DM, Botvinick MM, Noll D, Cohen JD (1998) Anterior cingulate cortex, error detection, and the online monitoring of performance. Science 280:747–749.

Davies MG, Rowan MJ, MacMathuna P, Keeling PW, Weir DG, Feely J (1990) The auditory P300 event-related potential: an objective marker of the encephalopathy of chronic liver disease. Hepatology 12:688–694.

Dehaene S, Kerszberg M, Changeux JP (1998a) A neuronal model of a global workspace in effortful cognitive tasks. Proc Natl Acad Sci USA 95:14529–14534.

Dehaene S, Dehaene-Lambertz G, Cohen L (1998b) Abstract representations of numbers in the animal and human brain. Trends Neurosci 21:355–361.

Dierks T, Maurer K (1990) Reference-free evaluation of auditory evoked potentials – P300 in aging and dementia. In: Early markers in Parkinson's and Alzheimer's disease (Dostert P, Riederer P, Strolin Benedetti M, Roncucci R, eds), pp. 197–208. Vienna: Springer-Verlag.

Dierks T, Khorram-Sefat D, Horn H, Syed N, Hacker H, Maurer K (1997) Functional magnetic resonance imaging (fMRI) of the auditory cortex during acoustical stimulation: a comparison to electrophysiological localization of late AEP. Electroenceph Clin Neurophysiol 103:42P.

Dierks T, Linden DEJ, Jandl M, Formisano E, Goebel R, Lanfermann H, Singer W (1999) Activation of Heschl's gyrus during auditory hallucinations. Neuron 22:615–621.

Elger CE, Grunwald T, Lehnertz K, Kutas M, Helmstaedter C, Brockhaus A, Van Roost D, Heinze HJ (1997) Human temporal lobe potentials in verbal learning and memory processes. Neuropsychologia 35:657–67.

Fylan F, Holliday IE, Singh KD, Anderson SJ, Harding GF (1997) Magnetoencephalographic investigation of human cortical area V1 using color stimuli. NeuroImage 6:47–57.

Gandhi SP, Heeger DJ, Boynton GM (1999) Spatial attention affects brain activity in human primary visual cortex. Proc Natl Acad Sci USA 96:3314–3319.

Goebel R, Khorram-Sefat D, Muckli L, Hacker H, Singer W (1998a) The constructive nature of vision: direct evidence from functional magnetic resonance imaging studies of apparent motion and motion imagery. Eur J Neurosci 10:1563–1573.

Goebel R, Linden DEJ, Lanfermann H, Zanella FE, Singer W (1998b) Functional imaging of mirror and inverse reading reveals separate coactivated networks for oculomotion and spatial transformations. NeuroReport 9:713–719.

Goodin DS, Squires KC, Starr A (1978) Long latency event-related components of the auditory evoked potential in dementia. Brain 101:635–648.

Halgren E, Baudena P, Clarke JM, Heit G, Liegeois C, Chauvel P, Musolino A (1995a) Intracerebral potentials to rare target and distractor auditory and visual stimuli: 1. Superior temporal plane and parietal lobe. Electroenceph Clin Neurophysiol 94:191–220.

Halgren E, Baudena P, Clarke JM, Heit G, Marinkovic K, Devaux B, Vignal J, Birabin A (1995b) Intracerebral potentials to rare target and distractor stimuli: 2. Medial, lateral and posterior temporal lobe. Electroenceph Clin Neurophysiol 94:229–250.

Halgren E, Marinkovic K, Chauvel P (1998) Generators of the late cognitive potentials in auditory and visual oddball tasks. Electroenceph Clin Neurophysiol 106:156–164.

Holmes A, Poline JB, Friston K (1997) Characterising brain images with the general linear model. In: Human brain function (Frackowiak RSJ, Friston K, Frith CD, Dolan RJ, Mazziotta JC, eds), pp. 59–84. San Diego: Academic Press.

Knight RT (1990) Neural mechanisms of event-related potentials: evidence from human lesion studies. In: Event-related brain potentials: basic issues and applications (Rohrbaugh JW, Parasuraman R, Johnson R Jr, eds), pp. 3–18. New York: Oxford University Press.

Knight RT, Nakada T (1998) Cortico-limbic circuits and novelty: a review of EEG and blood flow data. Rev Neurosci 9:57–70.

Knight RT, Scabini D, Woods DL, Clayworth CC (1989) Contributions of temporo-parietal junction to the human auditory P3. Brain Res 502:109–116.

Lehmann D, Skrandies W (1980) Reference-free identification of components of checkerboard-evoked multichannel potential fields. Electroenceph Clin Neurophysiol 48:609–621.

McCarthy G, Luby M, Gore J, Goldman-Rakic P (1997) Infrequent events transiently activate human prefrontal and parietal cortex as measured by functional MRI. J Neurophysiol 77:1630–1634.

Mecklinger A, Maess B, Opitz B, Pfeifer E, Cheyne D, Weinberg H (1998) A MEG analysis of the P300 in visual discrimination tasks. Electroenceph Clin Neurophysiol 108:45–56.

Menon RS, Kim S-G (1999) Spatial and temporal limits in cognitive neuroimaging with fMRI. Trends Cogn Sci 3:207–216.

Menon V, Ford JM, Lim KO, Glover GH, Pfefferbaum A (1997) Combined event-related fMRI and EEG evidence for temporal-parietal cortex activation during target detection. NeuroReport 8:3029–3037.

Oades RD, Walker MK, Geffen LB, Stern LM (1988) Event-related potentials in autistic and healthy children on an auditory choice reaction time task. Int J Psychophysiol 6:25–37.

O'Connor T, Starr A (1985) Intracranial potentials correlated with an event-related potential, P300, in the cat. Brain Res 339:27–38.

Paller KA, Zola-Morgan S, Squire L, Hillyard SA (1988) P3-like wave in normal monkeys and in monkeys with medial temporal lobe lesions. Behav Neurosci 102:714–725.

Paller KA, McCarthy G, Roessler E, Allison T, Wood CC (1992) Potentials evoked in human and monkey medial temporal lobe during auditory and visual oddball paradigms. Electroenceph Clin Neurophysiol 84:269–279.

Paus T, Koski L, Caramanos Z, Westbury C (1998) Regional differences in the effects of task difficulty and motor output on blood flow response in the human anterior cingulate cortex: a review of 107 PET activation studies. NeuroReport 9:R37–47.

Pfefferbaum A, Horvath TB, Roth WT, Kopell BS (1979) Event-related potential changes in chronic alcoholics. Electroenceph Clin Neurophysiol 47:637–647.

Picton T (1992) The P300 wave of the human event-related potential. J Clin Neurophysiol 9:456–479.

Polich J (1990) P300, probability, and interstimulus interval. Psychophysiology 27:396–403.

Polich J, Brock T, Geisler MW (1991) P300 from auditory and somatosensory stimuli: probability and inter-stimulus interval. Int J Psychophysiol 11:219–223.

Pritchard W (1986) Cognitive event-related potential correlates of schizophrenia. Psychol Bull 100:43–66.

Pritchard WS, Krieble KK, Duke DW (1996) Application of dimension estimation and surrogate data to the time evolution of EEG topographic variables. Int J Psychophysiol 24:189–195.

Puce A, Kalnins RM, Berkovic SF, Donnan GA, Bladin PF (1989) Limbic P3 potentials, localization and surgical pathology in temporal lobe epilepsy. Ann Neurol 26:377–385.

Ritter W, Vaughan Jr HG, Costa LD (1968) Orienting and habituation to auditory stimuli: a study of short-term changes in average evoked responses. Electroenceph Clin Neurophysiol 25:550–556.

Ritter W, Vaughan HG (1969) Average evoked responses in vigilance and discrimination: a reassessment. Science 164:326–328.

Rodin E (1991) P3 latency determination by global field power in normal subjects. J Clin Neurophysiol 8:88–94.

Roelfsema PR, Lamme VA, Spekreijse H (1998) Object-based attention in the primary visual cortex of the macaque monkey. Nature 395:376–381.

Scherg M, Linden DEJ, Muckli L, Roth R, Drüen K, Ille N, Zanella FE, Singer W, Goebel R (1999) Combining MEG with fMRI in studies of the human visual system. Adv Biomagnet (in press).

Smith DBD, Donchin E, Cohen L, Starr A (1970) Auditory averaged evoked potentials in man during seletive binaural listerning. Electroenceph Clin Neurophysiol 28:146–152.

Smith ME, Halgren E, Sokolik M, Baudena P, Musolino A, Liegeois-Chauvel C, Chauvel P (1990) The intracranial topography of the P3 event-related potential elicited during auditory oddball. Electroenceph Clin Neurophysiol 76:235–248.

Squires KC, Wickens C, Squires NK, Donchin E (1976) The effect of stimulus sequence on the waveform of the cortical event-related potential. Science 139:1142–1146.

Strik WK, Dierks T, Franzek E, Stober G, Maurer K (1994) P300 in schizophrenia: interactions between amplitudes and topography. Biol Psychiat 35:850–856.

Sutton S, Braren M, Zubin J, John ER (1965) Evoked potential correlates of stimulus uncertainty. Science 150:1187–1188.

Talairach J, Tournoux P (1988) Co-planar stereotaxic atlas of the human brain. New York: Thieme.

Tootell RB, Hadjikhani N, Hall EK, Marrett S, Vanduffel W, Vaughan JT, Dale AM (1998) The retinotopy of visual spatial attention. Neuron 21:1409–1422.

Vaughan HG, Ritter W (1970) The sources of auditory responses recorded from the human scalp. Electroenceph Clin Neurophysiol 28:360–367.

Watanabe T, Sasaki Y, Miyauchi S, Pütz B, Fujimaki N, Nielsen M, Takino R, Miyakawa S (1998) Attention-regulated activity in human primary visual cortex. J Neurophysiol 79:2218–2221.

Yamaguchi S, Knight RT (1991) Anterior and posterior association cortex contributions to the somatosensory P300. J Neurosci 11:2039–2054.

Yamaguchi S, Knight RT (1992) Effects of temporal-parietal lesions on the somatosensory P3 to lower limb stimulation. Electroenceph Clin Neurophysiol 84:139–148.

Yen SC, Finkel LH (1998) Extraction of perceptually salient contours by striate cortical networks. Vis Res 38:719–741.